Available online at www.sciencedirect.com
SCIENCE DIRECT®
Journal of Molecular Catalysis A: Chemical 237 (2005) 215–223
JOURNAL OF MOLECULAR CATALYSIS A: CHEMICAL
www.elsevier.com/locate/molcata

Dynamics and characterization of an innovative Raschig rings–TiO_2 composite photocatalyst

P. Raja [a], M. Bensimon [b], A. Kulik [c], R. Foschia [c], D. Laub [d], P. Albers [e], R. Renganathan [f], J. Kiwi [a,*]

[a] *Laboratory of Photonics and Interfaces, Institute of Chemical Sciences and Engineering, 1015 Lausanne, Switzerland*
[b] *Department of Civil Engineering, (GEOLEP), 1015 Lausanne, Switzerland*
[c] *Instiute of Physics of Complex Matter, 1015 Lausanne, Switzerland*
[d] *Institute of Electron Microscopy of Swiss Federal Institute of Technology, 1015 Lausanne, Switzerland*
[e] *AQura GmbH, D-63457, Hanau, Germany*
[f] *Department of Chemistry, Bharatidasan University, Tiruchirappalli, TN, India*

Received 4 March 2005; received in revised form 29 April 2005; accepted 29 April 2005
Available online 13 June 2005

Abstract

This study presents a novel supported photocatalyst on Raschig glass rings using polyethylene-graft-maleic anhydride (PEGMA) as a functionalized copolymer to fix TiO_2 Degussa P25 on the glass rings. The immobilized photocatalyst presented long-term stability and could be reused during the photodegradation of 4-chlorophenol (4-CP) without a loss in activity. Aqueous solution of 4-CP (0.49 mM or 35 mg C/L) at their natural pH of 5.6 and TiO_2 loaded Raschig rings showed complete decomposition of 4-CP within 5 min under irradiation with a medium pressure mercury lamp. The dependence of the 4-CP photodegradation was investigated as a function of: (a) gas atmosphere of the reaction, (b) concentration of the electron acceptor (H_2O_2), (c) initial concentration of 4-CP (d) intensity of the applied light and (e) pH of the solution. By X-ray photoelectron spectroscopy (XPS), the percentage of the elements and the binding energies (BE) was determined for the main elements on the catalyst surface. Scanning electron microscopy (SEM) determined a coating with variable a thickness of ∼100–300 nm on the glass rings. This is equivalent to a TiO_2 Degussa P25 coating of ∼10 layers thick. By atomic force microscopy (AFM) the increase in the roughness radius of TiO_2 pores was observed from 37.6 nm before use to 46.4 nm after use. This indicates that the catalyst pore diameter has increased as observed by AFM. The BET area of the sample was observed to increase from 29.4 m^2/g for the catalyst before use to 40.7 m^2/g for the TiO_2 Raschig glass rings samples after use.

Keywords: TiO_2/glass rings; Catalyst synthesis; 4-CP degradation; XPS; AFM; EM

1. Introduction

During the past decade, heterogeneous photocatalysis has been increasingly used in the preparation of fine chemicals and in water and air purification [1–3]. More than 1600 references have appeared during the last 10 years in reviewed journals where TiO_2 is used as a photocatalyst [4–7]. Two obstacles hinder the application of this semi-conductor TiO_2 in suspensions for the oxidative abatement of toxic and/or recalcitrant non-biodegradable compounds (a) the separation of the semiconductor after the process a step that is expensive in terms of manpower, time and energy (centrifugation or other form of separation) and (b) the low quantum yield of the process hindering the overall efficiency.

This study focuses on the stable fixation of TiO_2 on glass Raschig rings. Supported TiO_2 coated on glass has led in many cases to TiO_2 leaching into the solution during the photo-activated degradation of the pollutant [8,9]. This study presents an innovative route to anchor the TiO_2 powder suspension on glass rings using a negatively charged polyethylene-graft-maleic anhydride copolymer (PEGMA)

* Corresponding author. Tel.: +41 21 693 3621; fax: +41 21 693 4111.
E-mail address: john.kiwi@epfl.ch (J. Kiwi).

1381-1169/$ – see front matter © 2005 Elsevier B.V. All rights reserved.
doi:10.1016/j.molcata.2005.04.060

interface to anchor the positive TiO_2 on the surface of glass rings. The choice of Raschig rings was arrived at during the preliminary runs, when scanning different supports because it presented favorable kinetics and long-term stability as a support for particulate TiO_2 [10]. The photocatalyst fulfilled the following three requirements: (a) it did not degrade by the radicals produced in the solution necessary to degrade 4-CP, (b) it did not allow leaching of the TiO_2 during reactor operation and (c) it presented acceptable kinetics able to decompose 4-CP in the minutes range. This last property important due to the expensive UV-photons used during the degradation process.

TiO_2 anchoring on polyethylene block-copolymer films containing negatively charged anhydride groups has been reported by our laboratory [11]. TiO_2 nano-sized particles graft on the anhydride groups of the copolymer block polyethylene film. The anchoring of the TiO_2 goes through the carboxylic group interacting electrostatically with the Ti-cation and leading to the formation of the $-COO-Ti^{4+}$ bond. This study reports the coating with a negatively low cost commercial copolymer powder dissolved in an organic solvent in a solution that was used to coat the Raschig glass rings. Subsequently the thin polymer film on the rings with the anchoring groups was exchanged with TiO_2.

In recent years there has been a growing concern related to the health impact of chlorinated organic compounds. Chlorophenols constitute a group of organic substances that are introduced into the environment as result of man-made activities, such as wood preservatives, waste incineration, pesticide, herbicides and fungicides residues in water bodies. As of late, chlorocarbons found in water bodies are largely due to the bleaching of pulp with chlorine and the chlorination of water for disinfection purposes [12]. Chlorocarbons have been recognized as a threat to human health since their half-lives reach up to several years and have been listed in the 55 priority pollutants by the US EPA [13]. Therefore, the development of effective methods for their removal from water bodies is warranted. A recent comprehensive review article of Esplugas et al., [14] lists in Table 15 several studies using TiO_2 suspensions for 4-CP treatment and in some cases TiO_2 deposited on flat glass surfaces. Our laboratory has recently reported the degradation of chlorocarbons with TiO_2 suspensions under mercury light irradiation [15].

2. Experimental

2.1. Materials and reagents

The 4-chlorophenol (4-CP), acids, bases and H_2O_2 were Fluka p.a. and used as received. The TiO_2 Degussa P-25 photocatalyst was a gift from Degussa Switzerland, 6340 Baar. The Raschig rings used were 4 mm × 4 mm in size and were made out of soda lime glass 1 mm thick. The soda lime glass used was made up by: 70% SiO_2, 10% (Na_2O, CaO, MgO K_2O) and 5% (Fe_2O_3, Al_2O_3). The polyethylene-graft-maleic anhydride powder (PEGMA) was a Sigma-Aldrich product No. 456624, CAS Number 106343-08-2, melting point 107 °C, M_w 2300 (average molecular wt.). The structure of PEGMA is

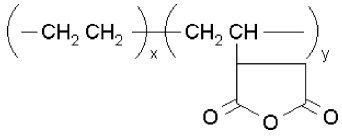

Other polyethylene-graft copolymers films were assayed as interfacial films to charge negatively the Raschig glass rings, but after preliminary scanning the one used beginning in Fig. 1 was selected. It showed the most suitable kinetics during the model organic compound used in this study.

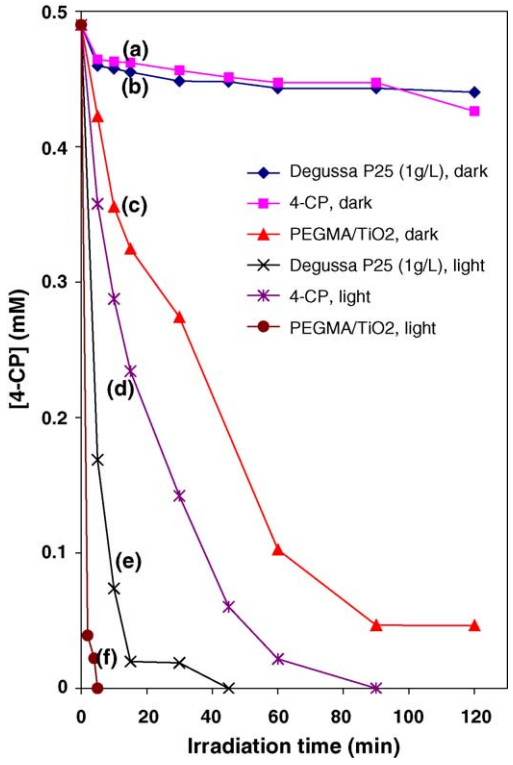

Fig. 1. Disappearance of 4-CP in aqueous solution as determined by HPLC in the dark and under mercury light irradiation (400 W) in the presence of H_2O_2 (10 mM) in air atmosphere. Initial solution at pH 5.6. The traces describing the catalysts are labeled from (a) through (f) in the captions. For other details see text.

2.2. Catalyst preparation

The Raschig rings were washed with detergent and then etched with HF 5%, for 10 min at 50 °C. After rinsing with bi-distilled water, the Raschig rings were immersed in the PEGMA 5% copolymers dissolved in toluene, drained and dried overnight in a vacuum oven. The dried rings were dipped in a well-dispersed TiO_2 Degussa P25 suspension (5 g/L) and dried at 110 °C for 1 h. The immersion in TiO_2 suspensions was repeated again to increase the TiO_2

deposition on the glass rings in areas that were not covered during the first dip coating. Then, the rings were heated at 100 °C in air for 1 h and subsequently for different time periods at 500 °C to eliminate the PEGMA interfacial coating agent.

Finally, the TiO_2 coated glass rings were washed again to eliminate the loosely bound TiO_2 particles. This is done by repeatedly shaking the Raschig loaded rings until no more TiO_2 flakes are seen to leach out of the glass surface. When the TiO_2 coating is too thick, sonication is applied for short times to eliminate TiO_2 that is not strongly attached to the glass surface.

The PEGMA binds the TiO_2 through the $-COO^-$ interacting electrostatically with the surface of TiO_2 in aqueous solution. The electrostatic attraction occurs between the $TiOH_2^+$ form in solution at pH 4.2 and the PEGMA negative $-COO^-$ groups. Further structural studies of the photocatalyst are not possible since the PEGMA interfacial agent is eliminated during the last step of the catalyst synthesis at 500 °C.

2.3. Irradiation procedures

The photodegradation of 4-CP was carried out in small batch cylindrical photochemical reactor made from glass (cutoff $\lambda = 265$ nm) containing 50 ml solution. An amount of 30 g TiO_2 Raschig rings was introduced in the reactor. The vessels were irradiated with a medium pressure mercury lamp (400 W) from Photochemical Reactor Ltd (Blounts Farm, Reading, Berkshire, UK) with a water-cooling jacket. The radiation field was 360° with 2.5×10^{19} photons/s. The integral radiant flux of the medium pressure mercury lamp reaching the reactor vessel wall was measured with a power-meter (YSI Corp. Colorado, USA). The incident light reaching the reactor wall was reduced by using iron-grid filters with mesh size diameters 0.15 and 0.6 mm.

2.4. Analyses of the irradiated solutions

The absorption of the solutions was followed in a Hewlett-Packard 38620 N-diode array spectrophotometer. The total organic carbon (TOC) was measured with a Shimadzu 5000 TOC analyzer. The disappearance of 4-CP was monitored with a high-pressure liquid chromatograph (HPLC) from Varian Corporation provided for with a 9065 diode. A Phenomenex C-18 inverse phase column was used in the HPLC and the gradient eluent solution consisted of a mobile phase of water (30%) and acetonitrile (70%). The peroxide concentration of the solutions were measured using Merckoquant® paper from Merck AG, Switzerland.

2.5. X-ray diffraction measurements

The crystallographic phase of the TiO_2 on the glass rings was measured with a Siemens X-ray diffractometer.

2.6. High resolution inductively coupled plasma spectrometry (ICPS)

The samples were acidified with nitric acid and diluted in ultrapure water to measure Ti^{4+}-ions in the irradiated solution. The ion-beam in the instrument plasma was directed through the sample and the accelerated into the mass analyzer. The collector assembly was a dual detector provided with a mass Faraday cup for the high beam current coupled with an electron multiplier for the low intensity signals.

2.7. X-ray photoelectron spectroscopy (XPS)

The XPS was performed using Mg Kα radiation. The electron energy analyzer (Leybold EA200) was operated at with band pass energy of 75 eV in the pre-selected transmission mode. Binding energies of the surface elements of interest were referenced to the $Au4f_{7/2}$ signal of 84.0 eV according to the SCA A83 standard of the National Physics Laboratory [16]. The evaluation of the binding energies (BE) for the most important elements of the catalyst surface was carried out following the standard procedures. A reproducibility of ±5% was attained in the XPS measurements. The ADS100 set was utilized to evaluate the XPS data by subtraction of X-ray satellites applying the background correction according to Shirley [17]. The presence of electrostatic charging effects was controlled by measurements including charge compensation by changing the electrostatic potential at the aperture site of the electron energy analyzer.

2.8. Scanning electron microscopy (SEM)

The scanning electron microscopy (SEM) was performed with a field emission gun (FEG) FEI XL30 Sirion SEM capable of a nominal resolution of 1 nm at 15 kV and 2 nm at 1 kV in secondary electron contrast mode. The cross sections of the surface of the rings were prepared for SEM by embedding the samples in an epoxy resin (Epon 810) and mechanical polishing with SiC paper using paper with a 5 μm granular structure. To avoid charging effects, the deposited samples were subsequently coated with a 20 nm gold layer. However, at the highest magnifications, the structure of the gold deposits interferes with that of the TiO_2 coating. The high-resolution SEM images were taken at 5 kV on uncoated chips of the TiO_2 deposits removed from the glass fiber by scratching from the glass using a razor blade to avoid excessive electric charge of the sample during the SEM work. Then this material was deposited on a carbon film positioned on a TEM Cu-grid.

2.9. Gas adsorption studies

Gas adsorption studies were carried out using a Sorptomatic 1900 micropore unit. The experiments were performed at liquid nitrogen boiling temperature (77 K). A reproducibility of 2% was attained during the determination of the

adsorption isotherms. The surface area of the samples was evaluated with the help of the data processing unit in the Micropore unit. To carry out the BET specific surface area determination of the TiO_2 before and after use, the TiO_2 was removed from the catalyst by sonication for 20 min in ethanol solution followed by drying at 110 °C.

2.10. Atomic force microscopy of TiO_2 loaded Raschig rings

The AFM images were obtained using an Atomic Force Microscope of AutoProbe M5 from ThermoMicroscopes Inc. The intermittent contact mode and silicon cantilever with conical tip was used having 13 N/m and resonant frequency 280 kHz. All scans were performed with a set-point amplitude of 25 nm and at a scanning rate 0.5 Hz. This insured stable tip radius and no sample wear during the experiments. Images were flattened by a line-by-line (3rd order polynomial fit) using Thermo Microscopes's image processing software. Consecutively, the roughness and bearing ratios were calculated.

3. Results and discussion

3.1. Photocatalytic screening of TiO_2 coated Raschig rings during 4-CP abatement

Preliminary runs were carried out using 4-CP (0.49 mM or 35 mg C/L) with TiO_2 coated Raschig glass ring prepared by using other copolymers than PEGMA like: poly (ethylene-co-ethyl acrylate-maleic anhydride), polypropylene-graft maleic anhydride, poly (styrene-alt-maleic anhydride) and poly (ethylene-alt-maleic anhydride). The most favorable 4-CP degradation kinetics was observed using PEGMA and this interfacial agent was selected for the photocatalyst used in this study.

Fig. 1 reports the results of runs in the dark and using a medium pressure mercury light irradiation in the presence of H_2O_2 (10 mM). Fig. 1(traces a, b) shows that the 4-CP degradation does not proceed in the dark in the absence or presence of Degussa TiO_2 P25. In the dark, the PEGMA/TiO_2 catalyst on Raschig rings is able to degrade 4-CP (trace c). The dark decomposition of 4-CP on the PEGMA/TiO_2 in Fig. 1 is due to the catalyst forming some oxidative species on the TiO_2 surface in the presence of H_2O_2. Under mercury light irradiation 4-CP is photodegraded (trace d). The initial photonic efficiency (ς) for (trace d) was estimated from the mercury light with 2.5×10^{19} photons/s reaching the front window of the reaction vessel within 4 min irradiation time. The value found was about 0.3. The 4-CP degradation under light and in the presence of H_2O_2 (10 mM) is possible since a 400 W mercury medium pressure lamp was used having emission lines from 230 nm and up to 450 nm. The 4-CP absorption spectrum begins at 304 nm and extends into the UV-C region. Therefore, 4-CP shows a region of absorption for the incoming light of the mercury light. The energy of the wavelengths in the UV-region is sufficient to break down chemical bonds in the molecular structure of 4-CP. Moreover, a modest decomposition of H_2O_2 will also take place and generates OH-radicals in solution active in the destruction of 4-CP.

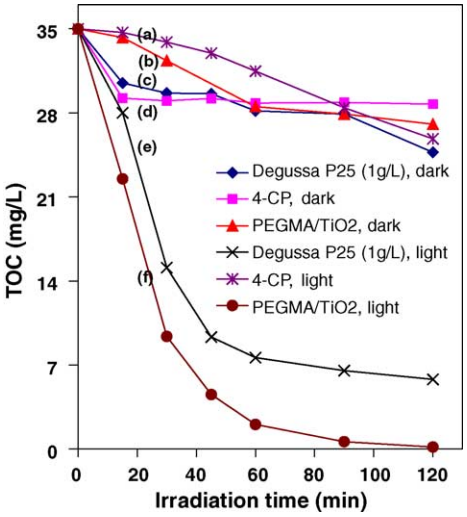

Fig. 2. TOC decrease of 4-CP in aqueous solution in the dark and under medium pressure mercury light irradiation in the presence of H_2O_2 (10 mM) in air atmosphere. Initial pH 5.6. The traces describing the catalysts are labeled from (a) through (f) in the captions.

The photodegradation reported in Fig. 1, trace e) in the presence of a suspension of Degussa TiO_2 P25 shows the favorable photocatalytic effect of the TiO_2 in suspension. In this case, the initial photonic efficiency was around 0.8. The photodegradation is even faster when adding PEGMA/TiO_2 (trace f) to the 4-CP solution and proceeds with a photonic efficiency of about 2.0.

The beneficial effect of the added H_2O_2 under light is due to its known electron acceptor role enhancing the charge separation at the TiO_2 surface

$$H_2O_2 + e_{cb}^- \rightarrow OH^- + OH^\bullet \quad (1)$$

Fig. 2 presents the decrease of TOC under the same experimental conditions as used to report the results presented in Fig. 1. It is readily seen that the TOC decrease involve reactions that proceed more slowly than the abatement of 4-CP as reported in Fig. 1. The PEGMA/TiO_2 supported on Raschig rings is seen to be more effective than when using suspensions of Degussa TiO_2 P25. This is due to the lower screening effect of 4-CP in the case of the PEGMA/TiO_2 supported on Raschig rings compared to the suspensions of Degussa TiO_2 P25 (1 g/l) allowing a better use of the applied light.

3.2. Effect of the H_2O_2 concentration, photocatalyst stability and effect of 4-CP concentration on the photodegradation kinetics

Fig. 3 shows the effect of the H_2O_2 concentration on the disappearance of 4-CP. It is readily seen that a concentra-

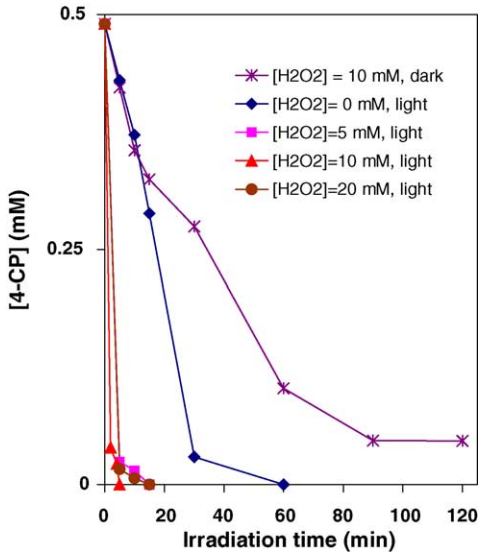

Fig. 3. Disappearance of 4-CP (0.49 mM) with initial pH 5.6 using PEGMA/TiO_2 glass rings under medium pressure mercury light as a function of the concentration of H_2O_2 added in solution.

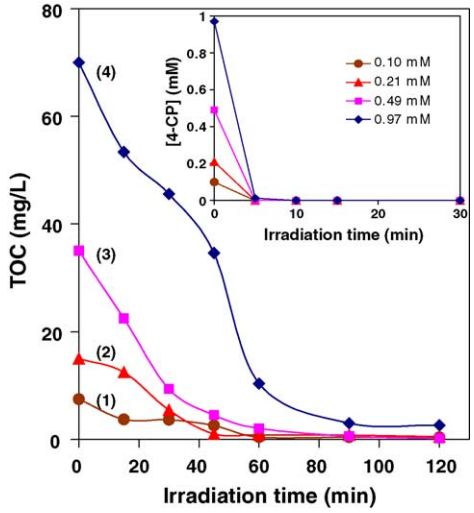

Fig. 4. TOC decrease of a 4-CP in solution as a function of the substrate concentration in solutions with initial pH 5.6 using PEGMA/TiO_2 glass rings under medium pressure mercury light. The insert shows the disappearance of 4-CP as a function of concentration.

tion of 5 mM H_2O_2 seems to be insufficient for the electron scavenging of the conduction band electrons produced upon irradiation on TiO_2. A concentration of 10 mM H_2O_2 accelerates the reaction but a higher concentration of H_2O_2 does not to increase the degradation kinetics. This is due to the scavenging of the OH-radical by the excess H_2O_2 in solution [1–3].

The catalyst performance when the catalyst is reused up to the sixth run did not change within the experimental error of the measurement. This shows the photo-stability of the PEGMA/TiO_2 glass rings. The Ti-ion concentration in solution was determined by ICPS up to the sixth repetitive recycling. For the reused catalyst, Ti-ions were observed in solution with a very low concentration < 0.3 mg/L.

Fig. 4 shows the TOC reduction of 4-CP solutions under mercury light irradiation for several 4-CP concentrations. Due to the shape of the TOC decrease seems to be a complex process involving long-lived intermediates. Fig. 4 (traces 1, 2 and 3) shows that the complete mineralization of 4-CP is reached within one hour. But the highest 4-CP concentration (trace 4) mineralized more inefficiently needing longer times. The insert in Fig. 4 shows that the 4-CP in the range 0.10–0.97 mM disappear within the same time (as far as this could be determined experimentally). This is an indication that a mass controlled process is taking place in the case of the three lower concentrations at the TiO_2 surface. The steeper decline observed at a higher 4-CP concentration is due to the more favorable mass transfer taking place between the 4-CP and the TiO_2 Raschig glass since the mass transfer between the solution and the photocatalyst is driven by the difference in 4-CP concentration between the bulk of the solution and the TiO_2 on the glass. The diffusion length (x) of the oxidative-radicals away from the glass rings can be estimated from the Smoluchowski diffusion relation

$$x^2 \sim Dt \quad (2)$$

The reaction rate between the $OH^\bullet$ radical and 4-CP has been reported to be close to $10^9\ M^{-1}\ s^{-1}$ [14]. At a concentration of 4-CP (0.20 mM), the lifetime of the encounter pair is $\sim 10^{-6}$ s. With $D \sim 5 \times 10^{-6}\ cm^2/s$, a value for the diffusion length (x) of ~50 nm Eq. (1) is found for the $OH^\bullet$ radical.

3.3. Light intensity dependence of 4-CP disappearance

Fig. 5 shows the disappearance of 4-CP as a function of light intensity as determined by HPLC. It is readily seen that

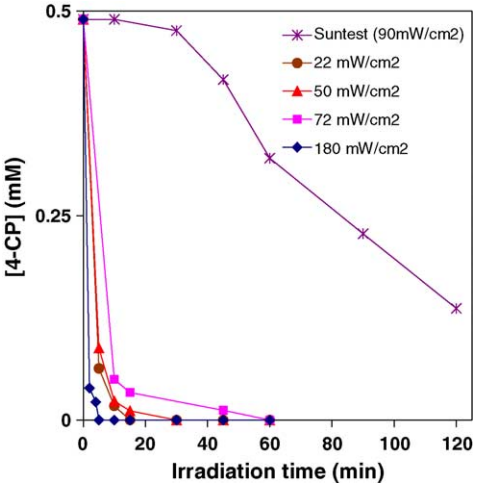

Fig. 5. Disappearance of 4-CP (0.49 mM) with initial pH 5.6 using PEGMA/TiO_2 glass rings under medium pressure mercury lamp irradiation as a function of the light intensity reaching the wall of the reaction vessel. The results obtained with a Suntest solar simulator are also shown for comparison purposes.

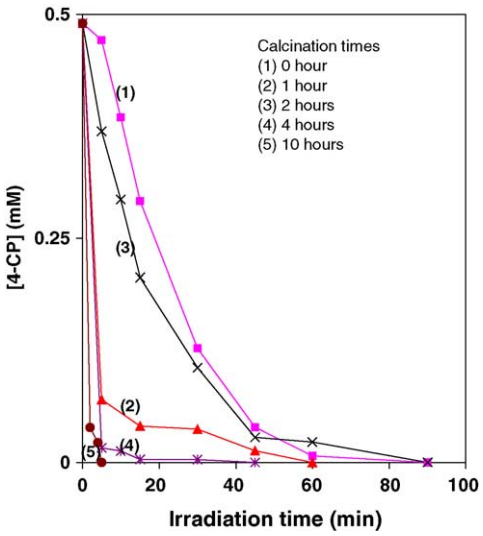

Fig. 6. Disappearance of 4-CP in solution in aqueous solution under medium pressure mercury lamp irradiation. Initial pH = 5.6 in air atmosphere. Calcinations times: Traces (1) no heating, (2) 1 h calcination at 500 °C (3) 2 h calcination at 500 °C (4) 4 h calcination at 500 °C and (5) 10 h calcination at 500 °C.

the 4-CP disappearance is more efficient as the intensity of the mercury applied light is increased. This implies that the saturation of TiO_2 acting as a photosensitizer has not been reached within the range of intensities tried. The flux of light used was decreased by using neutral gray grid filters (see Section 2). This reduced the number of incident photons reaching the wall of the reactor vessel. Also a Suntest solar simulator with 7% of the total photons below 400 nm was used as a source of flight. The photodegradation kinetics was seen to be lower compared to the mercury light source with a sharp peak at 366 nm.

3.4. Effect of the calcinations temperature on the 4-CP disappearance

Fig. 6 shows that the performance of the PEGMA/TiO_2 photocatalyst is a function of the calcination time at 500 °C. It is interesting to note in Fig. 6, that when no heating was applied during the catalyst preparation, a significant activity was still observed during the abatement 4-CP. During this study samples calcined for 10 h at 500 °C were used throughout.

3.5. The pH dependence of the 4-CP photodegradation

The pH values were seen to decrease during the 4-CP degradation and the final pH values shifted after 2 h from an initial pH 3.0 to 2.8, from 5.6 to 3.2 and from 7.0 to 4.7. The shift towards more acidic pH-values is due to the HCl generated during the overall degradation process

$$C_6H_5ClO + 13/2O_2 \rightarrow 6CO_2 + 2H_2O + HCl \quad (3)$$

The HCl in reaction (3) is due to the generation of the Cl^- anion in solution. This anion is produced due to the $TiO_2 e_{cb}^-$ under light irradiation reacting subsequently with 4-CP [14].

$$C_6H_5ClO + e_{cb}^- \rightarrow C_6H_5O^\bullet + Cl^-, \quad E^\circ = 0.8\text{–}1.2 \quad (4)$$

From Fig. 3 it is seen that when no H_2O_2 is added under light irradiation the 4-CP disappears after 60 min, and this can be ascribed to reaction (4). Fig. 3 also shows that an addition of H_2O_2 (10 mM) leads to a 4-CP disappearance after 5 min and this can be ascribed to reaction (1). Therefore, reaction (4) is highly favored for the e_{cb}^- under light irradiation for 4-CP solutions in the presence of H_2O_2.

3.6. X-ray diffraction (XRD) of the TiO_2 on glass rings

The X-ray diffraction shows rutile and anatase peaks for the TiO_2 of the PEGMA/TiO_2 glass rings. This is not surprising since TiO_2 Degussa P25 was employed in the preparation of the catalyst and calcined at 500 °C for 10 h.

3.7. X-ray photoelectron spectroscopy (XPS) of the catalyst used during 4-CP degradation

By XPS it is possible to determine the surface percentage of the elements in the ten top-most layers of the catalyst (about 20 Å). This is the penetration of the X-ray beam. Table 1 shows at time zero the XPS for the surface elements before the addition of 4-CP surface. Table 1 shows that the initial C, increases after 1 h during the 4-CP abatement but decreases considerably when all 4-CP was mineralized after 2 h reaction. The same behavior is observed for the Cl originating from 4-CP. This shows that the catalysis is efficient and does not allow the accumulation of C of 4-CP during the photocatalysis. The O-content increases during the treatment period due to the peroxide species produced by the TiO_2 under light irradiation. The surface percentages of Si, Na and K remain fairly constant during the treatment showing that Raschig glass rings retain a stable composition during the photocatalysis. The stable amount of Ti found during the treatment shows again the stability of the photocatalyst. Table 2 shows the binding energies (BE) of some of the elements found in the catalyst surface within the reaction time and C, N, O and Cl show almost constant BE values within the treatment time. The Ti 2p doublet shifts 0.3 eV. This is due to the fact that the relative amounts of TiOH groups and

Table 1
Percentage of elements at the catalyst surface

Spectrum line XPS	Initial $t = 0$	Middle $t = 1$ h	Final $t = 2$ h
C 1s	19.3	23.8	13.5
N 1s	0.22	0.14	0.19
O 1s	57.0	50.0	62.1
Na 1s	6.70	9.48	5.52
Si 2p	10.7	10.6	12.7
Cl 2p	0.06	0.21	0.13
K $2p_{3/2}$	0.27	0.11	0.10
Ti 2p	3.15	2.99	3.11

Table 2
Binding energy of some surface elements

Spectrum line XPS	Initial $t = 0$	Middle $t = 1$ h	Final $t = 2$ h
C 1s	286.0	285.9	286.0
N 1s	399.0	400.0	399.4
O 1s	535.7	535.8	535.9
Cl 2p	199.0	199.5	200.0
Ti 2p	460.8	460.8	460.5

adsorbed humidity change within the time of treatment. No asymmetric lower binding energy edge of the Ti 2p band was observed. It is suggested that no redox reaction in TiO_2 leading to the formation of a stable Ti^{3+}-species occurs due to the e_{cb}^- in TiO_2.

3.8. Scanning electron microscopy (SEM) of PEGMA/TiO_2 on glass rings

Fig. 7 shows the surface of the PEGMA/TiO_2 round glass rings. The SEM observation of the TiO_2 Degussa P25 particles removed from the glass rings showed sizes between 25 and 35 nm. The TiO_2 particle seen as dark spots of about 0.1–0.3 μm thick can be seen in a more detailed way in Fig. 8 close to the border of the glass rings. The darker gray area in Fig. 8 corresponds to the epoxy that entered the empty spaces of the glass ring surface.

3.9. Atomic force microscopy (AFM) of PEGMA/TiO_2 on glass rings

Fig. 9 shows the AFM study of a projected area of 10 μm × 10 μm for the PEGMA/TiO_2 catalysts before use.

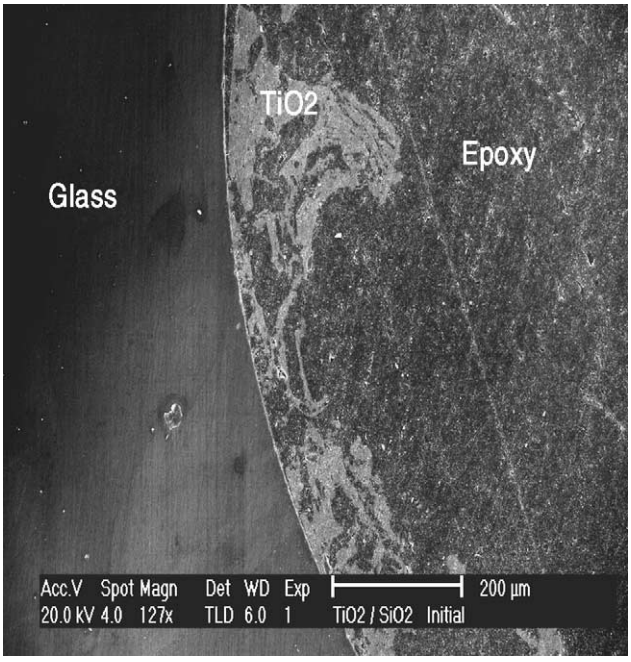

Fig. 7. Scanning electron microscopy (SEM) of the TiO_2 particles on the round Raschig glass ring surface for the PEGMA/TiO_2 glass rings.

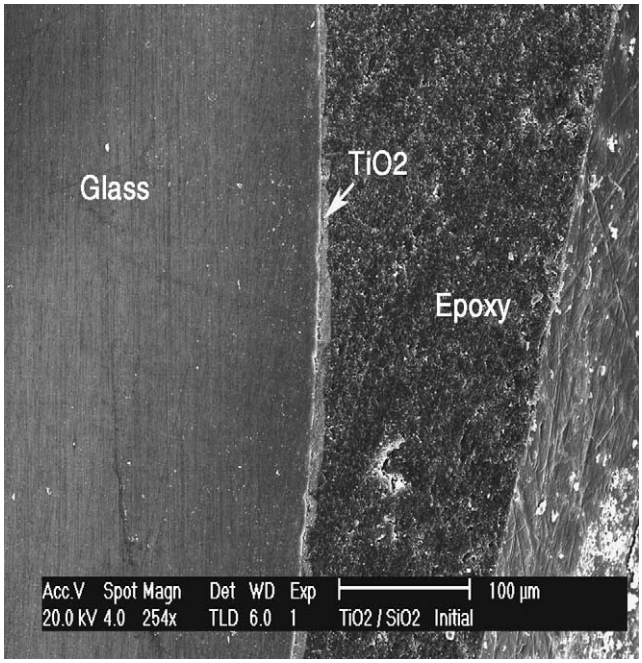

Fig. 8. Detailed structure by SEM of the PEGMA/TiO_2 glass rings.

This allows to make a relative a morphological interpretation of the catalyst surface since we account for the distance between the highest point and the lowest point in the TiO_2 film. The height of the TiO_2 layer is plotted up to 4000 pixels. The *x*-axis shows the distribution of the peak heights. The peak heights are shown in the *y*-axis. The histogram shows an rms roughness (root mean square-value) of 37.6 nm for the unused sample of PEGMA/TiO_2. The bearing ratio (expression in percentage of the histogram) was divided in three zones as shown by the broken lines in the histograms. The first zone (from the left) shows a Bearing ratio of 20% corresponding to an rms value of 185.5 nm extending up to the first broken vertical line. The middle zone includes the peak maximum up to 155.2 nm for a Bearing ratio of 50%. Finally, a bearing ratio of 80% corresponds to an rms value of 123.9 nm. For the samples of PEGMA/TiO_2 after use the roughness value were observed to increase to 46.4 nm meaning that the active surface of the sample increased modestly after use.

3.10. BET and porosity measurements of PEGMA/TiO_2 on glass rings before and after use

The BET for samples before use were determined after removing by sonication the TiO_2 powder from the Raschig glass rings in methanol media. Then, the suspension was dried and the amount of TiO_2 determined measuring the BET area in a Sorptomatic unit. The specific surface area (BET) for samples before use was 29.4 m^2/g and after use 40.7 m^2/g. The Barret, Joyner and Halenda (BJH) desorption cumulative surface of pores from 1 to 500 × 10^6 nm was calculated between 35 and 40 m^2/g for the samples before and after use [18].

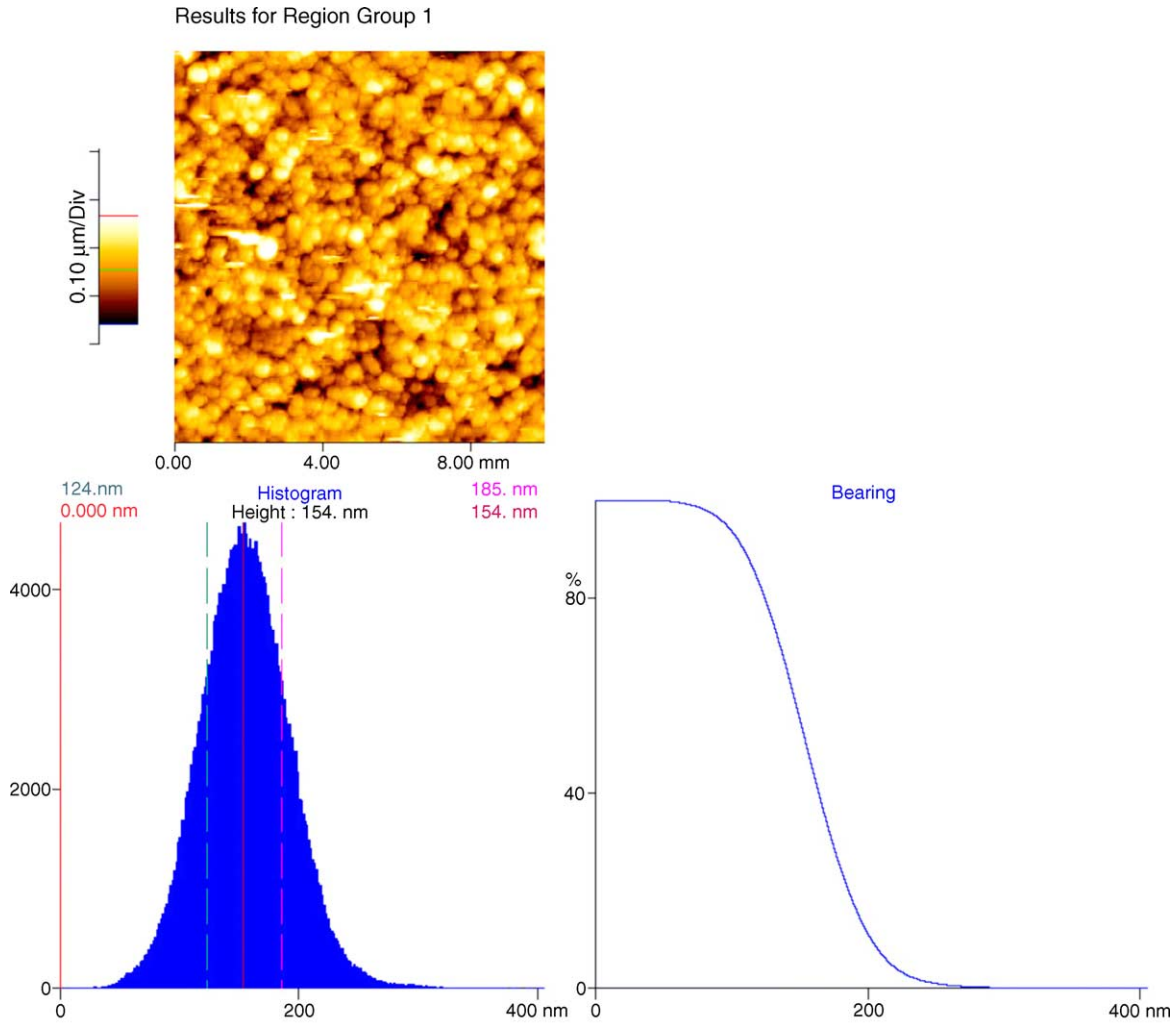

Rp-v	Rms Rought (Rq)	Ave Rought (Ra)	Mean Ht	Median Ht	Bearing Ratio	Bearing Ratio
405.5 nm	37.61 nm	29.55 nm	155.2 nm	154.4 nm	@20.0% 185.52 nm	@80.0% 123/95 nm
Peak (Rp)	Valley (Rv)	Volume	Surface Area	Projected Area		
250.4 nm	-155.2 nm	15.52 µm³	109.2 µm²	100.0 µm²		

Fig. 9. Atomic force microscopy observation for TiO_2/Raschig glass rings before use.

4. Conclusions

A new type of preparation for TiO_2 on glass Raschig rings has been presented in detail. The catalyst preparation was dependent on the interfacial copolymer type used to coordinate and electrostatically bind TiO_2 to the glass surface as found during the preliminary screening of a series of different aliphatic acids. The PEGMA/TiO_2 photocatalyst showed stable catalytic performance during long-term 4-CP degradation under mercury lamp irradiation. This stability is important, since this photocatalyst can be applied avoiding TiO_2 powders separation from a suspension in waste water decontamination processes. Since the 4-CP abatement proceeded within minutes, the process had an acceptable kinetic rate. No organic deposit was observed on the catalyst surface as observed by XPS during 4-CP photodegradation. This is a proof for the efficiency of the PEGMA/TiO_2 catalyst used that does not require separation at the end of the 4-CP abatement, allowing reuse without further treatment.

Acknowledgments

We gratefully acknowledge the financial support of CTI TOP-NANO 21 under Grant No. 5960.1 (Bern, Switzerland) and of the COST D-19 Program under grant No. CO 2.0068.

References

[1] Th. Oppenlaender, Photochemical Purification of Water and Air, Wiley-VCH, Weinheim Germany, 2003.
[2] A. Fujishima, K. Hashimoto, T. Watanabe, TiO_2 Photocatalysis, Fundamentals and Applications, Bkc, Inc., Tokyo, Japan, 1999.
[3] D.F. Ollis, H. Al-Ekabi, Photocatalytic Purification and Treatment of Water and Air, Elsevier, Amsterdam, 1993.
[4] A. Mills, S. Lee, Photochem. Photobiol. A 152 (2002) 233–249.
[5] A. Mills, S. Lehunte, Photochem. Photobiol. A 108 (1997) 1–11.
[6] R. Bauer, G. Waldner, S. Hager, S. Malato, P. Maletzky, Catal. Today 53 (1999) 131–139.
[7] L. Lucarelli, V. Nadtochenko, J. Kiwi, Langmuir 16 (1999) 1102–1117.
[8] U. Stattford, A. Gray, P.V. Kamat, J. Phys. Chem. 98 (1994) 6343–6348.
[9] K. Hofstadler, R. Bauer, S. Novalic, G. Heisler, Environ. Sci. Technol. 28 (1994) 670–676.
[10] A. Bozzi, J. Kiwi, Appl. Catal. B 20 (2004) 201–209.
[11] M.R. Dhanajeyan, E. Mielczarski, K. Thampi, Ph. Buffat, M. Bensimon, A. Kulik, J. Mielczarski, J. Kiwi, J. Phys. Chem. B 105 (2001) 12046–12065.
[12] U.G. Ahlborg, T.M. Thandberg, CRC Crit. Rev.Toxicol. 53 (1999) 131–137.
[13] L.H. Keith, W.A. Telliard, Environ. Sci. Technol. 13 (1979) 416–423.
[14] M. Pera-Titus, V. Garcia-Molina, M. Banos, J. Gimenez, S. Esplugas, Appl. Catal. B 27 (2004) 219–235.
[15] J. Bandara, J. Mielczarski, A. Lopez, J. Kiwi, Appl. Catal. B 34 (2001) 321–328.
[16] D. Briggs, M. Shea, Practical Surface Analysis, vol. 1, 2nd ed., John Wiley, Chichester, UK, 1990.
[17] A. Shirley, Phys. Rev. B 5 (1979) 4709–4717.
[18] P. Barret, L. Joyner, P. Halenda, J. Am. Chem. Soc. 73 (1951) 1371–1378.